High-order harmonic generation in fullerenes with icosahedral symmetry

M. F. Ciappina* and A. Becker†
Max-Planck-Institut für Physik komplexer Systeme, Nöthnitzer Strasse 38, D-01187 Dresden, Germany

A. Jaroń-Becker†
Institut für Physikalische Chemie und Elektrochemie, Technische Universität Dresden, D-01062 Dresden, Germany
(Received 26 August 2008; published 3 December 2008)

We investigate high-order harmonic generation in a sequence of icosahedral fullerenes using the extension of the so-called three-step or Lewenstein model to the molecular case. The high harmonic spectra obtained at midinfrared wavelengths show modulations in the plateau region. These modulations are due to the coherent superposition of the contributions from the atomic centers in the molecule to the dipole moment. Results of test calculations, in which the interference effects between the atomic contributions are deliberately neglected, show a "flat" plateau, as it is known from high-order harmonic generation in atoms. It is shown that the characteristic modulations are present in ensembles of aligned fullerenes as well as randomly oriented ones. We further show that in the case of the larger fullerenes the radius can be determined from the positions of the interference minima in the high harmonic spectra using a spherical model.

DOI: 10.1103/PhysRevA.78.063405 PACS number(s): 33.80.Rv, 33.80.Wz, 42.50.Hz

I. INTRODUCTION

One of the most interesting phenomena that appear as a consequence of the nonlinear interaction between intense laser fields and atoms or molecules is high-order harmonic generation (HHG). This process refers to the transformation of a large number of laser photons into a single high-frequency photon. Besides its fundamental nature as a process of frequency conversion, HHG has recently attracted interest as a source to obtain information about the structure of a molecule on an ultrafast time scale (for a recent review, see, e.g., [1]). This prospect of HHG becomes obvious from the so-called rescattering or three-step model of HHG [2,3]. In the first step of the sequence, the system (atom or molecule) is field ionized by the strong linearly polarized laser field; in the second, the free electron is accelerated by the oscillating electric field of the laser pulse: first away from and then back to the parent ion. Finally, as the electron returns back to the positively charged core, it can recombine under emission of a high-frequency photon. It is well known that both ionization of a molecule [4] and coherent emission of harmonic light due to the recombination process [5] strongly depend on the symmetry of the molecular orbital involved as well as on the orientation or alignment of the molecule with respect to the polarization axis. Furthermore, it has been shown recently that vibrational dynamics of nuclei within a molecule can be resolved via observation of high harmonic spectra [6–9]. It is therefore feasible to use HHG as a "camera" to observe changes in the molecular structure on (sub-)angstrom and (sub-)femtosecond scales. In this respect HHG may, to some extent, become an alternative to other well-known tools of determination of molecular structure, such as ultrafast electron diffraction [10,11], laser-induced electron diffraction [12,13], or diffractive x-ray imaging with free-electron lasers [14].

Several investigations in recent years have confirmed that information about the molecular structure and the orbital symmetries can be obtained from high harmonic spectra. First, characteristic minima in the HHG spectra of H_2^+ and H_2, as observed in the results from numerical simulations [5,15–18], have been interpreted as due to a coherent addition of the dipole amplitudes from the atomic centers in diatomic molecules. In strong fields the interference concept between partial amplitudes is also known for electron emission as an explanation for the phenomenon of suppressed molecular ionization [4,19–21]. In the case of HHG, however, it has been established that there exists a correlation between the interference minima in the recombination matrix element and those in the HHG spectra. In the experiment the two-center interference effect has been first observed in the harmonic signal of CO_2 [22,23]. One of the most exciting examples toward molecular imaging via HHG has been the proposal of the molecular orbital tomography method and its application to N_2 [24]. The theoretical basis and prospects of the tomography technique have been investigated and discussed vigorously [25–31].

In order to evaluate the potential of molecular imaging it is important to study HHG from large polyatomic molecules. In this respect, molecular structure effects in the harmonic signal from aligned organic molecules have been observed in the experiment recently [32]. Furthermore, interference minima have been identified in theoretical results obtained for the emission of high-order harmonics from the C_{60} fullerene [33]. Most interestingly, it has been shown that for this highly symmetric molecule the interference pattern does not disappear for an ensemble of randomly oriented fullerenes. In contrast, in the case of all other molecules studied before, an alignment of the molecule has been found to be an essential condition to observe interferences and retrieve structural information.

*Present address: Institute of High Performance Computing, 1 Fusionopolis Way, #16-16 Connexis, Singapore 138632.
†Present address: Department of Physics and JILA, University of Colorado, 440 UCB, Boulder, CO 80309, USA.

It is the goal of the present paper to extend our previous investigations on HHG in the C_{60} fullerenes [33] to another set of fullerenes with icosahedral symmetry, namely, C_{20}, C_{80}, and C_{180}. For the calculation of the harmonic signal in these fullerenes we have employed the extension of the so-called Lewenstein model, originally proposed for HHG in atoms [34], to the molecular case. Since computations within this model take much less computational effort than *ab initio* simulations, they are particularly useful for studies in complex molecules, such as the icosahedral fullerenes. In the Lewenstein model the time-dependent dipole moment in an intense laser field is evaluated by considering the transition of the electron from the ground state of an atom (or molecule) to the Volkov states [35]. Transitions to excited bound states and the Coulomb interaction of the electron with the ion in the continuum as well as multichannel effects are neglected within this model. Using the so-called single active electron (SAE) approximation, in which it is assumed that just one electron becomes active during the response to the external field, the Lewenstein model can be extended to deal with HHG in multielectronic atoms and molecules.

We organize the paper as follows. In Sec. II we briefly sketch the Lewenstein model for high-order harmonic generation in complex molecules including the geometrical structure and orbital symmetry of the molecule. We then will present and discuss the results of our numerical calculations for high-harmonic generation in the sequence of icosahedral fullerenes C_{20}, C_{80}, and C_{180}, obtained at (near-infrared and) midinfrared laser wavelengths. A comparison between the HHG response for ensembles of aligned and randomly oriented fullerenes will be presented as well. We will further study how structural information can be retrieved from the interference patterns present in the harmonic spectra using a spherical model. The paper ends with a short summary.

II. LEWENSTEIN MODEL FOR HIGH-ORDER HARMONIC GENERATION IN COMPLEX MOLECULES

In order to evaluate HHG spectra in molecules, we make use of the quantum-mechanical version of the three-step model, which has been originally proposed by Lewenstein *et al.* for atoms [34]. The most widely used version of this model is based on an expression for the time-dependent dipole moment $\mathbf{D}(t)$ due to the response of a single atom or molecule to the laser field within the SAE approximation. The dipole acceleration $\mathbf{a}(t)$ is then calculated as (Hartree atomic units, $e=m=\hbar=1$ are used)

$$\mathbf{a}(t) = \ddot{\mathbf{D}}(t), \tag{1}$$

and the HHG spectrum is obtained by modulus squaring the Fourier transform of the dipole acceleration, i.e.,

$$S(\omega) \sim |\mathbf{a}(\omega)|^2, \tag{2}$$

where $\mathbf{a}(\omega)=\int_0^{T_p} dt \mathbf{a}(t)\exp(i\omega t)$ for a laser pulse with a finite duration time T_p. The time-dependent dipole moment of the molecule can then be written as (e.g., [36])

$$\mathbf{D}(t) = -i\int_0^t dt' \int d^3k \mathbf{d}_{\mathrm{rec}}^*(\mathbf{k}+\mathbf{A}(t),\{\mathbf{R}\}_j) \times d_{\mathrm{ion}}^{(L)}(\mathbf{k}+\mathbf{A}(t'),\{\mathbf{R}\}_j;t')\exp[-iS(\mathbf{k},t,t')] + \mathrm{c.c.}, \tag{3}$$

where $S(\mathbf{k},t,t')=\int_{t'}^t dt''\{[\mathbf{k}+\mathbf{A}(t'')]^2/2+I_p\}$ represents the semiclassical action, where I_p is the ionization potential of the molecule, and $\mathbf{A}(t)=-c\int_{-\infty}^t \mathbf{E}(t')dt'$ is the vector potential of the linearly polarized laser field $\mathbf{E}(t)$. We have performed the three-dimensional integration over $\mathbf{k}$ in Eq. (3) using the saddle-point or stationary phase method, while all time integrations are performed numerically. Since the intensity of the harmonics is strongest for polarization along the direction of the linearly polarized laser field, we have considered the contribution in this direction only.

In Eq. (3) we have made explicit the dependence of the dipole moment on the orientation of the molecule via the coordinates of the nuclei, $\{\mathbf{R}\}_j$. In the present work we have performed calculations using ensembles of aligned and randomly oriented icosahedral fullerenes (C_{20}, C_{80}, and C_{180}). The latter are performed by averaging the modulus squared of the dipole acceleration over different orientations of the fullerenes.

The ionization and recombination amplitudes in Eqs. (3) are given in length gauge by

$$d_{\mathrm{ion}}^{(L)}(\mathbf{k},\{\mathbf{R}\}_j;t) = \langle \phi_0(\mathbf{k},\mathbf{r})|\mathbf{E}(t)\cdot\mathbf{r}|\Phi_i(\mathbf{r},\{\mathbf{R}\}_j)\rangle, \tag{4}$$

and

$$\mathbf{d}_{\mathrm{rec}}(\mathbf{k},\{\mathbf{R}\}_j) = \langle \phi_0(\mathbf{k},\mathbf{r})|-\mathbf{r}|\Phi_i(\mathbf{r},\{\mathbf{R}\}_j)\rangle, \tag{5}$$

respectively. $\phi_0(\mathbf{k},\mathbf{r})$ is a plane wave of momentum $\mathbf{k}$ and $\Phi_i(\mathbf{r},\{\mathbf{R}\}_j)$ is the undressed initial state orbital of the active electron in the molecule. Angular brackets denote integration over the coordinates of the electron. The multicenter nature of the molecule, its geometric structure, and the orbital symmetry of the active orbital are taken into account in the representation of the orbital as a linear combination of atomic orbitals (LCAO), $\phi_{j,l}(\mathbf{r},\{\mathbf{R}\}_j)$, centered at the nuclear positions $\mathbf{R}_j$, $j=1,2,\ldots,M$.

$$\Phi_i(\mathbf{r},\{\mathbf{R}\}_j) = \sum_{j=1}^{M}\sum_{l=1}^{l_{max}} a_{j,l}\phi_{j,l}(\mathbf{r},\mathbf{R}_j), \tag{6}$$

where M is the number of the nuclei in the molecule, $a_{j,l}$ are the variational coefficients of the atomic functions, and l_{max} is the size of the basis set used. For the present purpose of evaluating high harmonic spectra in the icosahedral fullerenes C_{20}, C_{80}, and C_{180}, we have acquired its geometrical structure using the density-functional tight-binding method [37–39]. The atomic orbitals are then obtained using the self-consistent Hartree-Fock method with Gaussian basis functions [40]. In all cases we have restricted ourselves to study the HHG response from the highest occupied molecular orbital (HOMO). The differences in binding energies of the HOMO and the HOMO-1 are 10% or more and range between 0.7 eV (C_{180}) and 1.7 eV (C_{20}) at the Hartree-Fock level adopted.

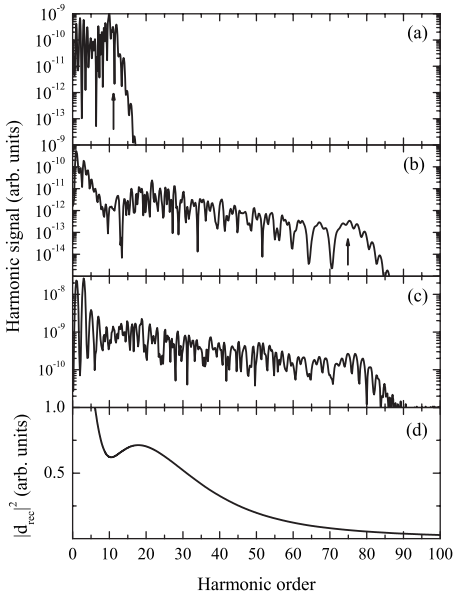

FIG. 1. HHG spectra for an ensemble of aligned C_{20} molecules at (a) $\lambda=800$ nm and (b) $\lambda=1800$ nm and a peak laser intensity of $I_0=5\times10^{13}$ W/cm^2, a pulse duration of 30 fs, and a sin^2-pulse shape. (c) Same as panel (b) but neglecting the interference effects in the matrix elements, (d) Recombination matrix element as a function of the harmonic order n using the relation $n\omega_{1800}=k^2/2+I_p$ with $\omega_{1800}=0.0253$ a.u. ($\lambda=1800$ nm) and $I_p^{C_{20}}=0.255$ a.u. (6.94 eV).

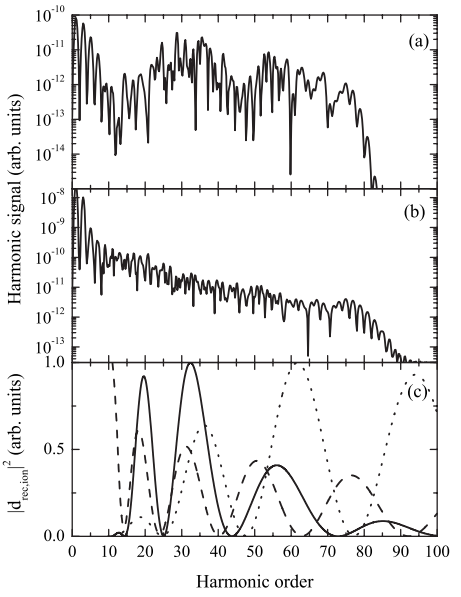

FIG. 2. HHG spectra for an ensemble of aligned C_{80} molecules at $\lambda=1800$ nm. (a) Full calculation. (b) Incoherent sum calculation. The other laser parameters are as in Fig. 1. (c) Comparison of the recombination transition matrix element (solid line) with the predictions of the spherical model based on cosine functions [dashed line, Eq. (7)] and with the spherical model based in spherical Bessel functions [dotted line, Eq. (9)]. The recombination matrix element is plotted as a function of the harmonic order n using $n\omega_{1800}=k^2/2+I_p$ with $\omega_{1800}=0.0253$ a.u. ($\lambda=1800$ nm) and $I_p^{C_{80}}=0.246$ a.u. (6.69 eV).

III. HIGH-ORDER HARMONIC YIELDS FROM FULLERENES WITH ICOSAHEDRAL SYMMETRY

We have performed calculations for HHG spectra in a sequence of icosahedral fullerenes, namely, C_{20}, C_{80}, and C_{180} at different wavelengths of the laser field. The goal of our investigation is to identify distinct interference patterns in the spectra for these fullerene species and to confirm that the interference features are present even in an ensemble of randomly oriented fullerenes with a highly symmetric atomic frame, as it has been found in our previous results for the C_{60} fullerene [33].

As in the case of the C_{60} fullerene, the observation of the characteristic interference patterns requires high-order harmonic generation at midinfrared laser wavelengths. This can be seen immediately from the comparison of the high harmonic spectra for C_{20} at (a) 800 nm and (b) 1800 nm, shown in Fig. 1. Both spectra have been obtained for a pulse with a peak intensity of $I_0=5\times10^{13}$ W/cm^2, a pulse duration of 30 fs, and a sin^2-pulse shape. Please note that, here as well as in all the other cases below, the peak intensity has been chosen to be close but below the respective saturation intensity of the neutral fullerene for both wavelengths (cf. [20]). Before proceeding we may note parenthetically that the spectra show the expected sharp cutoff, which is in good agreement with the predictions of the semiclassical three-step model [marked by small arrows in panels (a) and (b)]. There is no unphysical extension of the plateau, as it has been found in numerical simulations using the length gauge for diatomic molecules with large internuclear distances [36]; we may therefore conclude that the length gauge formulation of the Lewenstein model is applicable in the present case.

In order to identify the, if any, interference structures in the spectra we have first considered an ensemble of C_{20} molecules in which the main symmetry axis is aligned along the polarization axis of the laser. While the spectra at 800 nm do not show any specific modulation due to the short plateau [Fig. 1(a)], we observe a pronounced minimum in the strength of the harmonics at about $n=9$ at a driving wavelength of 1800 nm [Fig. 1(b)]. Such features have been seen and interpreted before in the case of C_{60} as due to a multislit interference effect between the contributions from the different atomic centers to the dipole moment [33]. Consequently, we expect that the minimum will disappear when the contributions from the 20 C atoms are summed up incoherently in the calculation of the dipole moment, i.e., neglecting the interference terms. This is indeed the case as the corresponding results in Fig. 1(c) show. The harmonic spectrum does not show any modulation but is "flat" as it is known from high-order harmonic generation in atoms.

As discussed at the outset, in diatomic molecules there exists a close correlation between the zeros in the recombination matrix element and the position of the minima in the harmonic spectrum [1,5]. The same holds in the case of the C_{20} fullerene, which can be seen from the comparison of the recombination matrix element in Fig. 1(d) and the harmonic spectrum in Fig. 1(b).

In order to proceed, we further analyze to which extent interference patterns are present in the HHG spectra for C_{80}

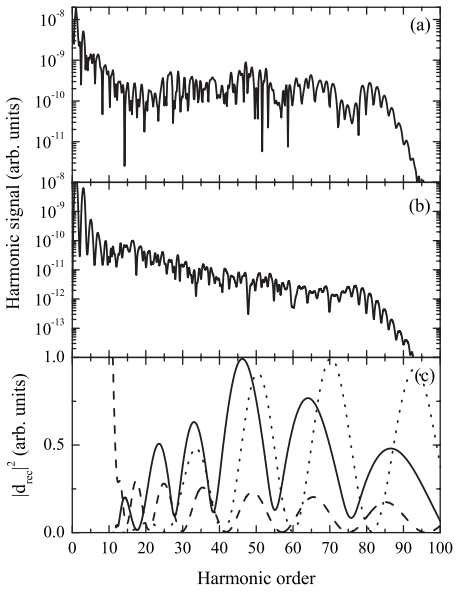

FIG. 3. Same as Fig. 2 but for an ensemble of aligned C_{180} fullerenes with $I_p^{C_{180}}=0.272$ a.u. (7.4 eV).

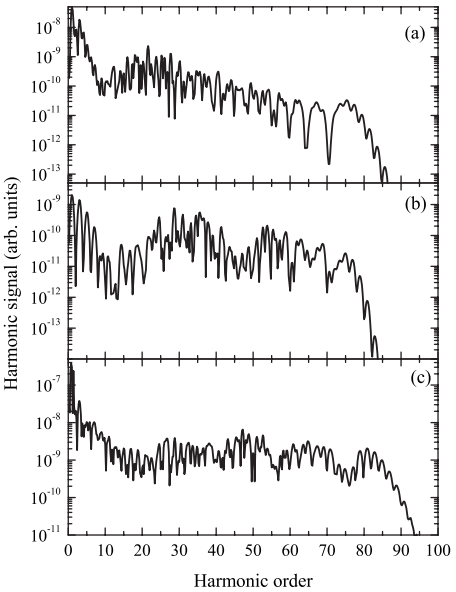

FIG. 4. HHG spectra for ensembles of randomly oriented fullerenes at $\lambda=1800$ nm. (a) C_{20}, (b) C_{80}, and (c) C_{180}. The other laser parameters are as in Fig. 1.

and C_{180}. Indeed, they are clearly visible in the corresponding results presented in panels (a) of Fig. 2 (C_{80}) and Fig. 3 (C_{180}). In both cases we have again first considered ensembles of aligned molecules, in which the main symmetry axis is aligned along the polarization axis, to clearly identify the interference minima. In both cases the interference patterns observed are much richer than in the case of C_{20}. The characteristic minima in the spectra are found to correspond once more with those in the recombination matrix element [solid lines in panels (c)]. The evidence that the origin of the modulations in both spectra is due to the multislit interference effects is confirmed by comparison with the results of the respective test calculations, in which we have deliberately neglected the contribution of the interference terms in the matrix elements [shown in Figs. 2(b) and 3(b)]. The high-harmonic spectra, calculated via the incoherent sum of the atomic contributions, show, as before, a flat plateau without any evidence of a minimum.

Before we discuss the results presented by the dashed and dotted lines of Figs. 2(c) and 3(c) in Sec. IV we first clarify if the interference patterns analyzed above show up in ensembles of randomly oriented fullerenes too. As expected from our previous study on C_{60} [33], for the present fullerenes with icosahedral symmetry, an average of the spectra over the orientation of the fullerenes with respect to the polarization does not "wash out" the interference minima in the plateaus of the spectra. The corresponding results are plotted in Fig. 4 for the C_{20} [panel (a)], C_{80} [panel (b)], and C_{180} [panel (c)], respectively. The interference patterns are clearly visible in all the cases.

IV. DETERMINATION OF THE RADIUS OF THE FULLERENE FROM THE HIGH HARMONIC SPECTRA

In the case of C_{60} we have analyzed how the radius of the fullerene can be obtained from the position of the interference minima in the high-harmonic spectra [33]. To this end, we had derived an approximative expression for the recombination matrix element using a model, in which the initial state is approximated by a simple spherical-shell-like state $\Phi_i(\mathbf{r},\{\mathbf{R}\}_j)=\Theta_R(r)Y_{l_i,m_i}(\hat{\mathbf{r}})$. In this approximation the modulus square of the recombination transition amplitude (5) can be written as

$$|\hat{\mathbf{e}}\cdot\mathbf{d}_{\mathrm{rec}}(\mathbf{k},\{\mathbf{R}\}_j)|^2 \propto \left|\sum_{l_f,m_f} Y_{l_f,m_f}(\hat{\mathbf{k}})(-i)^{l_f} \times \int j_{l_f}(kr)\Theta_R(r)r^3dr \times \int Y_{l_f,m_f}(\hat{\mathbf{r}})\hat{\mathbf{e}}\cdot\hat{\mathbf{r}}Y_{l_i,m_i}(\hat{\mathbf{r}})d\hat{\mathbf{r}}\right|^2, \quad (7)$$

with

$$\Theta_R(r)=\begin{cases}-V_0, & R-\Delta\leq r\leq R\\ V_0, & R\leq r\leq R+\Delta\\ 0, & \text{otherwise},\end{cases} \quad (8)$$

where $R=\frac{1}{N}\sum_{j=1}^{N}|\mathbf{R}_j|$ and Δ are the radius of a spherical shell and the half width of the shell, respectively,

$$V_0^2=\frac{1}{2R^2\Delta}\left(1+\frac{\Delta^2}{3R^2}\right)^{-1},$$

$l_f=l_i\pm1$, and N is the number of C atoms in the fullerene. $\Theta_R(r)$ is an approximation of the initial state wave function of the fullerenes by a spherical shell-like state (e.g., [41]). The approximation accounts for the icosahedral symmetry of the fullerenes in a simple way. Equation (7) can be further simplified as

TABLE I. Comparison of the radii of C_{80} and C_{180} as obtained from the geometrical structure calculations (R) and as retrieved from the positions of the interference minima in the harmonic spectra (n_i) using the spherical model expressions (7) and (9).

	Fullerene radius (a.u.)		
Species	R	Using Eq. (7)	Using Eq. (9)
C_{80}	7.71	7.71 (n_1=25)	7.44 (n_1=25)
		8.15 (n_2=43)	7.38 (n_2=43)
C_{180}	11.345	10.72 (n_1=27)	10.81 (n_1=27)
		11.83 (n_2=39)	11.92 (n_2=39)
		12.02 (n_3=55)	11.59 (n_3=55)
		11.92 (n_4=75)	11.35 (n_4=75)

$$|\hat{\mathbf{e}}\cdot\mathbf{d}_{\mathrm{rec}}(\mathbf{k},\{\mathbf{R}\}_j)|^2 \propto \frac{V_0^2}{k^2}\left[\int_R^{R+\Delta}\cos\left(kr-\frac{l_i}{2}\pi\right)r^2dr - \int_{R-\Delta}^{R}\cos\left(kr-\frac{l_i}{2}\pi\right)r^2dr\right]^2 \quad (9)$$

by approximating the spherical Bessel function j_l by trigonometric functions and neglecting the angular terms in m_i and m_f, which are irrelevant for the further analysis. The asymptotic expression for the spherical Bessel functions is expected to hold for $kr \approx kR > 2l_i$ (e.g., [42]).

The predictions of both expressions of the spherical model are plotted in panels (c) of Figs. 2 and 3, for C_{80} and C_{180}, respectively [dotted line, Eq. (7); dashed line, Eq. (9)]. We have used l_i=6 for C_{80} and l_i=9 for C_{180} [43], and the respective radii obtained from the geometrical structure calculations (cf. Table I). Since the results are found to be rather independent of the choice of Δ we have therefore assumed Δ=0.95 as in our previous C_{60} calculations [33].

From the comparison in Figs. 2(c) and 3(c) one sees that the model predictions agree rather well with each other and the results of the full recombination matrix element. As it has been pointed out before [33], the spherical model can be used to retrieve the radius of the fullerene from the positions of the interference minima in the harmonic spectra, actually even below the limit for the asymptotic expression of the Bessel function ($n_i > 58$ for C_{80} and $n_i > 61$ for C_{180}). The corresponding results, using both the model formulas (7) and (9), are compared in Table I with the actual radius used in the calculations of the high-harmonic spectra. It is seen that the predictions deviate less than 10% from the actual radius and may therefore serve as an alternative tool to obtain characteristic structural information from high harmonic spectra generated in large molecules with almost spherical symmetry.

V. CONCLUSIONS

We have studied high-order harmonic generation from a sequence of fullerenes with icosahedral symmetry interacting with a linearly polarized intense laser pulse. Calculations of the spectra are performed using an extension of the Lewenstein model to the molecular case. The spectra for all the species show distinct modulations in the plateau region for driving laser wavelengths in the midinfrared (but not in the near-infrared regime). The modulations are found to be due to a multislit interference effect arising from the coherent contributions of the different atomic centers to the electronic dipole moment. We have further shown that the interference minima in the harmonic spectra can be correlated to the minima in the recombination matrix elements and do appear in ensembles of aligned as well as randomly oriented fullerenes due to the high symmetry of the nuclear cage. Finally, we have shown that it is possible to infer the radius of the fullerene from the interference minima present in the harmonic spectra using a spherical model for the recombination matrix element.

[1] M. Lein, J. Phys. B **40**, R135 (2007).
[2] P. B. Corkum, Phys. Rev. Lett. **71**, 1994 (1993).
[3] K. J. Schafer, B. Yang, L. F. DiMauro, and K. C. Kulander, Phys. Rev. Lett. **70**, 1599 (1993).
[4] J. Muth-Böhm, A. Becker, and F. H. M. Faisal, Phys. Rev. Lett. **85**, 2280 (2000).
[5] M. Lein, N. Hay, R. Velotta, J. P. Marangos, and P. L. Knight, Phys. Rev. Lett. **88**, 183903 (2002).
[6] M. Lein, Phys. Rev. Lett. **94**, 053004 (2005).
[7] S. Baker, J. S. Robinson, C. A. Haworth, H. Teng, R. A. Smith, C. C. Chirilă, M. Lein, J. W. G. Tisch, and J. P. Marangos, Science **312**, 424 (2006).
[8] N. L. Wagner, A. Wuest, I. P. Christov, T. Popmintchev, X. Zhou, M. M. Murnane, and H. C. Kapteyn, Proc. Natl. Acad. Sci. U.S.A. **103**, 13279 (2006).
[9] Z. B. Walters, S. Tonzani, and C. H. Greene, J. Phys. B **40**, F277 (2007).
[10] H. Ihee, V. A. Lobatsov, U. M. Gomez, B. M. Goodson, R. Srinivasan, C.-Y. Ruan, and A. H. Zewail, Science **291**, 458 (2001).
[11] D.-S. Yang, C. Lao, and A. H. Zewail, Science **321**, 1660 (2008).
[12] T. Zuo, A. D. Bandrauk, and P. B. Corkum, Chem. Phys. Lett. **259**, 313 (1996).
[13] M. Meckel, D. Comtois, D. Zeidler, A. Staudte, D. Pavicic, H. C. Bandulet, H. Pépin, J. C. Kieffer, R. Dörner, D. M. Villeneuve and P. B. Corkum, Science **320**, 1478 (2008).
[14] H. N. Chapman *et al.*, Nat. Phys. **2**, 839 (2006).
[15] M. Lein, N. Hay, R. Velotta, J. P. Marangos, and P. L. Knight, Phys. Rev. A **66**, 023805 (2002).
[16] M. Lein, J. P. Marangos, and P. L. Knight, Phys. Rev. A **66**, 051404(R) (2002).
[17] G. LagmagoKamta and A. D. Bandrauk, Phys. Rev. A **70**, 011404(R) (2004).
[18] G. L. Kamta and A. D. Bandrauk, Phys. Rev. A **71**, 053407 (2005).

[19] J. Muth-Böhm, A. Becker, S. L. Chin, and F. H. M. Faisal, Chem. Phys. Lett. **337**, 313 (2001).
[20] A. Jaroń-Becker, A. Becker, and F. H. M. Faisal, Phys. Rev. Lett. **96**, 143006 (2006).
[21] A. Jaroń-Becker, A. Becker, and F. H. M. Faisal, J. Chem. Phys. **126**, 124310 (2007).
[22] T. Kanai, S. Minemoto, and H. Sakai, Nature (London) **435**, 470 (2005).
[23] C. Vozzi, F. Calegari, E. Benedetti, J.-P. Caumes, G. Sansone, S. Stagira, M. Nisoli, R. Torres, E. Heesel, N. Kajumba, J. P. Marangos, C. Altucci and R. Velotta, Phys. Rev. Lett. **95**, 153902 (2005).
[24] J. Itatani, D. Zeidler, J. Levesque, M. Spanner, D. M. Villeneuve, and P. B. Corkum, Phys. Rev. Lett. **94**, 123902 (2005).
[25] R. Santra and A. Gordon, Phys. Rev. Lett. **96**, 073906 (2006).
[26] R. Santra, Chem. Phys. **329**, 357 (2006).
[27] W. H. Eugen Schwarz, Angew. Chem. **45**, 1508 (2006).
[28] S. Patchkovskii, Z. X. Zhao, T. Brabec, and D. M. Villeneuve, Phys. Rev. Lett. **97**, 123003 (2006).
[29] S. Patchkovskii, Z. X. Zhao, T. Brabec, and D. M. Villeneuve, J. Chem. Phys. **126**, 114306 (2007).
[30] J. Levesque, D. Zeidler, J. P. Marangos, P. B. Corkum, and D. M. Villeneuve, Phys. Rev. Lett. **98**, 183903 (2007).
[31] V.-H. Le, A.-T. Le, R.-H. Xie, and C. D. Lin, Phys. Rev. A **76**, 013414 (2007).
[32] R. Torres, N. Kajumba, J. G. Underwood, J. S. Robinson, S. Baker, J. W. G. Tisch, R. deNalda, W. A. Bryan, R. Velotta, C. Altucci I. C. E. Turcu, and J. P. Marangos, Phys. Rev. Lett. **98**, 203007 (2007).
[33] M. F. Ciappina, A. Becker, and A. Jaroń-Becker, Phys. Rev. A **76**, 063406 (2007); **78**, 029902(E) (2008).
[34] M. Lewenstein, P. Balcou, M. Y. Ivanov, A. L'Huillier, and P. B. Corkum, Phys. Rev. A **49**, 2117 (1994).
[35] D. M. Wolkow, Z. Phys. **94**, 250 (1935).
[36] C. C. Chirilă and M. Lein, Phys. Rev. A **73**, 023410 (2006).
[37] D. Porezag, T. Frauenheim, T. Kohler, G. Seifert, and R. Kaschner, Phys. Rev. B **51**, 12947 (1995).
[38] G. Seifert, D. Porezag, and T. Frauenheim, Int. J. Quantum Chem. **58**, 185 (1996).
[39] M. Elstner, D. Porezag, G. Jungnickel, J. Elsner, M. Haugk, T. Frauenheim, S. Suhai, and G. Seifert, Phys. Rev. B **58**, 7260 (1998).
[40] *Gaussian03, Revision C.02* (Gaussian, Inc., Wallingford, CT, 2004); URL http://www.gaussian.com
[41] S. Hasegawa, T. Miyamae, K. Yakushi, H. Inokuchi, K. Seki, and N. Ueno, Phys. Rev. B **58**, 4927 (1998).
[42] A. Messiah, *Quantum Mechanics* (Wiley, North Holland, 1976).
[43] M. S. Dresselhaus, G. Dresselhaus, and P. C. Eklund, *Science of Fullerenes and Carbon Nanotubes* (Academic Press, San Diego, 1996).